Renewable Energy 254 (2025) 123716

Contents lists available at ScienceDirect

Renewable Energy

journal homepage: www.elsevier.com/locate/renene

Best tilt of PV system in Canada: Effect of the sky radiation model and climate conditions

Samuele Memme [a], Marco Fossa [a,*], Daniel Rousse [b]

[a] DIME - Department of Mechanical, Energy, Management and Transportation Engineering, University of Genova, Italy
[b] Groupe t3e – Département de génie mécanique, École de technologie supérieure, Montréal, Canada

ARTICLE INFO

Keywords:
Photovoltaic solar energy
Best tilt angle
Clearness index
Irradiance modelling
Snow albedo

ABSTRACT

This paper focuses on the best tilt angle of photovoltaic applications, to be related to the latitude and a latitude correction factor here presented. The analysis includes a series of 19 cities across Canada: latitude and local weather conditions are considered to define a correction angle correlation. This correction is expressed as a function of latitude, average annual weather conditions, and yearly climate variability, demonstrating strong alignment with "exact" outputs (correlation coefficient equal to 0.98 for different sky models). To ensure broad geographic coverage, Typical Meteorological Year hourly data were obtained from the Canadian Weather Year for Energy Calculation portal. The validity of the correction was assessed against various approaches and web tools results. Results were then compared with those from European cities at similar latitudes. Findings indicate that determining the optimum tilt angle requires accounting for latitude and site-specific climatic conditions, including snow cover: snowy regions benefit from higher tilts, emphasizing the relevance of considering accurate albedo in photovoltaic system design. Results suggest that this precise tilt calculation can yield annual insolation gains of up to 3.5 % with respect to rule-of-thumb angles (i.e. tilt equal to latitude), even at lower latitudes, with variations in best tilts until 13°.

Nomenclature

Greek letters	
α_s	Solar elevation angle [°]
β	Tilt angle [°]
γ	Azimuth angle of the surface[°]
γ_s	Solar azimuth angle [°]
δ	Declination solar angle [°]
$\Delta\varphi$	Latitude correction factor [°]
θ_s	Solar zenith angle [°]
θ_w	Angle of incidence [°]
μ	Average
ρ	Ground albedo
σ	Standard deviation
φ	Latitude [°]
ω	Hour angle [°]
Subscripts	
b	Beam
diff	Diffuse
H	Horizontal surface
HD	Hay and Davies
HDKR	Hay, Davies, Klucher and Reindl
LJ	Liu and Jordan
o,H	Extra-terrestrial on horizontal
opt	Optimum
ref	Ground-reflected
s	Summer average
ss	Sunset
sr	Sunrise
tot	Total
T	Tilted surface
w	Winter average
y	Yearly average
Superscripts	
d	Day
m	Month
Acronyms	
CWEC	Canadian Weather Year for Energy Calculation
PV	Photovoltaic
TMY	Typical meteorological year
Symbols	
H	Insolation [kWh/m^2/hour] or [kWh/m^2/day] or [kWh/m^2/y]
K_t	Clearness index
r	Correlation coefficient
R_b	Beam radiation tilt factor

(*continued on next column*)

(*continued*)

* Corresponding author.
E-mail address: marco.fossa@unige.it (M. Fossa).

https://doi.org/10.1016/j.renene.2025.123716
Received 5 November 2024; Received in revised form 22 May 2025; Accepted 8 June 2025
Available online 9 June 2025

1. Introduction

In recent years, energy scenarios have seen a rise in sustainable conversion technologies and growing interest in distributed power generation. This trend is driven by national and international policies addressing the climate crisis, alongside the need to diversify energy sources and reduce foreign dependence. As a result, the adoption of solar technologies, including photovoltaic (PV) systems and thermal collectors, has steadily increased. Due to their widespread diffusion, PV applications play a crucial role, accounting for a global installed capacity of 1183 GW as of 2022: as the 2023 IEA Report states, more than half of this capacity has been deployed in the preceding four years, bearing witness to the rapid and recent widespread adoption of such systems on a large scale [1]. Moreover, the cost of electric energy from PV sources can be nowadays considered comparable to that from conventional fossil-based production, with world-average Levelized Cost of Electricity (LCOE) of PV plants reduced by 89 % from 2010 to 2022, according to IRENA report [2]. In this context, the problem of maximizing the utilization of solar resources has become of crucial interest and a series of strategies can be adopted to this end. In particular, regarding fixed solar installations, it is often convenient to investigate the optimum slope to maximize the annual cumulative insolation on the solar receiving surface. Several correlations exist in the literature to estimate radiation components based on measured or calculated global values. Modelling diffuse sky insolation, over a specified time, or instantaneous irradiance, on inclined surfaces is critical when direct measurements are unavailable. In these cases, tilted surface insolation is estimated using transposition models, which convert horizontal data into tilted values. This process involves a transposition factor, a non-dimensional ratio that adjusts for solar position and system geometry, representing the relationship between tilted and horizontal insolation values [3].

The estimation of the optimum fixed tilt angle of surfaces requires a series of local insolation data. The latter can be derived from ground measurements. Alternatively, they can be determined using geostationary satellite data, able to cover a wide portion of land: this solution avoids the need for constant calibration of ground sensors and provides a continuous coverage of land, without the need for a large number of high-quality stations. In the literature, some approaches focus on maximizing beam insolation on tilted surfaces. As a general guideline, this method can be considered reliable for locations between 5° and 40° latitude characterized by particularly sunny climates, as demonstrated by Yadav et al. in Ref. [4]: for such latitudes, the beam component of solar radiation is significantly higher than the diffuse one. It is then calculated using the well-established Liu and Jordan isotropic model [5]: according to this approach, the diffuse solar radiation is described as uniformly distributed across the sky. Similar conclusions were drawn by Bailek et al. in Ref. [6], where an experimental setup was used to assess the best tilt based on the Perez model [7]: this is among the most recognized anisotropic models, i.e. those accounting for variations in diffuse radiation due to factors like cloud cover, atmospheric scattering, and solar position. Many authors investigated the disagreement between yearly tilts according to different isotropic and anisotropic models. Among these, Shukla et al. [8] and Calabrò [9] considered several empirical models, highlighting that the two approaches give similar results during summer; on the other hand, they differ the most at lower declination angles, when the investigated anisotropic models provide values up to 9° higher than the isotropic one. The higher accuracy of anisotropic models is further stressed in Ref. [10] by Padovan et al., with particular reference to the cases in which diffuse irradiance measurements are not available. The authors stress that the case of surfaces oriented away from the south, it requires the combined use of transposition models and diffuse fraction correlations. Posadillo et al. [11] compared distinct models for diffuse irradiance, highlighting the higher accuracy of anisotropic approaches to determine insolation on a tilted surface. A detailed analysis of different transposition models is also presented in Ref. [12] by Raptis et al.: their accuracy has been assessed against a full year of irradiance measurements. Results showed higher insolation values for horizontal surfaces during summer and cloudy winter days with respect to tilted ones; moreover, the authors pointed out that the best azimuthal orientation of a surface is also dependent on when the maximum performance is required during the day. González-González et al. [13] estimated the production losses due to non-optimum fixed tilt angles relying on latitude-dependent correlations for best tilt calculations in the Iberian peninsula. The effect of such arrangements is even more obvious when urban constraints impose an azimuth orientation different than due south, as reported by both Barbón et al. [14], Yadav et al. [15] and Ebhota et al. [16].

Often, the next step after identifying the optimum tilt angle involves determining analytical relationships to calculate this angle based on one or more independent variables. When the model is based on relationships expressed as a function of latitude only, it does not capture and describe those average weather factors that can affect solar irradiance. This results in the calculation of the same tilt angles for any location based at the same latitude. The simplest of these correlations, i.e. tilt angle equal to the latitude itself, is considered in the study by Bailek et al. [6] based on the Perez model [7]. A similar approach was taken by Moghadam et al. in Ref. [17], with optimum tilt angles derived for two cities at latitudes 29.49° N and 27.18° N: linear regression revealed a strong dependence of tilt angle on latitude, suggesting that negative angles may be needed in case of daily adjustments. Further studies, such as those of Chang [18] and Luque and Hegedus [19], propose linear latitude-tilt correlations for predicting optimum angles, while Khosravi et al. [20] extend these findings to locations in both hemispheres for flat plate collectors. However, it should be highlighted that in these studies a tilt angle equal to the latitude is close to the yearly best one only under clear sky conditions. These studies do not account for the impact of diffuse radiation and its contribution to global insolation. As a general comment, the models used to account for the diffuse component play a significant role in the overall prediction of solar energy recovery.

Numerous authors have carried out more in-depth research into the dependence between best inclination and latitude. Talebizadeh et al. [21] considered fixed tilts but also daily and monthly slope adjustments: this approach allowed to estimate the accuracy of linear analytical relationships based on insolation data series with respect to reference data by Nijegorodov et al. [22]. Darhmaoui et al. [23] determined yearly optimum tilt based on 4-year daily global insolation for Mediterranean areas: their analysis of latitude-tilt correlation indicated that other climate factors have minimal impact. Several authors have proposed polynomial relations based on latitude to estimate the optimum tilt angle. Santos-Martin et al. [24] introduced a second-degree polynomial with coefficients depending on whether irradiance data come from clear-sky models or measurements. Chinchilla et al. [25] used irradiance data from the Baseline Surface Radiation Network (BSRN) and EnergyPlus to derive coefficients for a third-degree polynomial that fits optimum tilt angles for 2603 locations worldwide. Another cubic polynomial model is presented by Jacobson et al. [26], who used NREL's PVWatts tool to determine optimum tilt angles globally. The authors also evaluated the performance of static systems with annual optimum tilt versus various tracking options, emphasizing the role of tracking systems in locations with similar latitudes but different aerosol and cloud conditions. A similar analysis, i.e. aimed at determining the varying energy output based on the frequency of tilt adjustment, was presented by Abdallah et al. [27] for south-facing surfaces in Palestine, resulting in yearly optimum tilts approximately 2° lower than the local latitude. Likewise, Skeiker [28] compared different variable tilt strategies with a fixed annual one, finding that the yearly best tilt in Damascus, Syria, is about 3° lower than the latitude. Benghanem [29] calculated a tilt just 1° lower than the latitude for Madinah, Saudi Arabia. Daily, monthly and annual tilts were for various locations in Iran by Abdolzadeh et al. [30]. For a broader overview of tilt adjustment and tracking strategies in monofacial and bifacial PV systems, the reader may refer to the detailed review by Sadeghi et al. [31].

When determining the daily optimum tilt angle, correlations based on the declination angle can be used. Bakirci [32] employed this approach, developing polynomials based on the solar declination angle to estimate the diffuse insolation on inclined surfaces. Similar studies include that of Tiris et al. [33], which highlights the accuracy of declination-based equations compared to clearness index; similarly, Kallioglu et al. [34] introduce monthly optimum tilt angle relations based on declination, comparing them with latitude-based polynomials. In Ref. [35], a polynomial using the month number as the variable is proposed for monthly optimum tilt by Garni et al., while Sharma et al. [36] developed polynomial models based on declination for the Western Himalayas. A similar declination-based third-degree polynomial was validated with long-term insolation data in Iraq by Hassan et al. [37]. A different method was used by Stanciu et al. [38], whose global correlations were developed by comparing isotropic and anisotropic models: according to their findings, the difference between latitude and local declination is a good predictor for the best tilt. Lastly, an analytical model for mid-latitude zones is proposed in Ref. [39] by Soulayman et al., taking into account latitude, declination and sunrise/sunset angles to evaluate the best tilt adjustment strategies.

Many of the above-mentioned models are limited to specific geographic areas often not accounting for local climate variables. To address this issue, more general models consider the clearness index, which affects the diffuse radiation component. Yang et al. [40] proposed a correlation for the optimum tilt angle based solely on the clearness index, assuming a constant value throughout the year. Liu et al. [41] developed models incorporating latitude and the diffuse fraction, showing strong agreement with empirical data from satellites and ground measurements. Elsayed [42] combined in a complex equation clearness index, latitude, and day of the year using historical insolation data to predict monthly and yearly optimum tilt, including surface azimuth influence. Jafarkazemi et al. [43] considered Iran to assess the influence of not only latitude but also average weather conditions on yearly best tilt. For tropical regions, Soulayman and Sabbagh [44] presented a nonlinear equation where the optimum tilt is latitude minus a correction factor based on day number, sunset hour, and declination angles. A similar approach was applied in Bangladesh [45] by Mamun et al. Yadav and Chandel [46] developed 12 quadratic polynomial correlations for 26 cities in India to maximize insolation on tilted surfaces. Wenxian [47] considered the ratio of beam to global insolation and latitude to derive a theoretical equation for optimum tilt. Finally, Christensen et al. [48] introduced a climate correction factor to adjust latitude for optimum tilt estimation in the U.S.: the authors considered latitude, yearly clearness index, and the ratio of winter to summer clearness indices, with a correction factor of zero at the equator under clear sky conditions.

Although PV tilt angle optimization has been widely studied, as highlighted in this introduction, a comprehensive analysis encompassing the entire Canadian territory remains absent, although works like the one by Barbón et al. [49] do include some of the cities analyzed in this research. Additionally, the impact of different diffuse sky models on best tilt calculations and annual solar insolation has not been thoroughly assessed. This study focuses on estimating the optimal tilt angles for PV applications across Canada and proposing an analytical correlation for their calculation tailored to its specific climate conditions. Additionally, it quantifies the effect of snow cover on albedo, evaluating how its inclusion or exclusion influences both optimal tilt angles and available solar energy: although albedo-dependent tilts are usually defined for bifacial PV [50], in snow-prone regions, the best tilt for monofacial ones could be affected by ground albedo as well. In the following, Section 2 provides an overview of the required theoretical background about diffuse sky models (Section 2.1), the mathematical modelling of an analytical correlation for PV best tilts (Section 2.2), and an overview of the online tools used for the present analysis (Section 2.3). A detailed description of the selected cities and input data is presented in Section 3. Results, presented in Section 4, include yearly insolation from different sky models (Section 4.1), and a comparison between the resulting best tilts and those from online resources (Section 4.2): provided that the goal is to maximize yearly insolation onto a tilted surface, the solar energy available can increase up to 3.5 % with respect to the usual latitude-based approach for medium-latitude cities, and even more (4.5 %–7.1 %) for high latitude ones. The proposed correlation for the analytical calculation of the best tilt as a function of latitude and climate conditions indicators is presented in Section 4.3. The same correlations have been used in the past for studying PV best tilts in Europe, and a comparison between the two case studies is provided in Section 4.4. Finally, the analysis has been further refined in Section 4.5 by assessing the impact of a variable albedo on the surface optimal slope and available insolation, highlighting changes in the tilts up to 5° at medium-latitude cities.

2. Methods

In this paper, the optimum tilt for fixed PV systems is calculated with reference to a series of Canadian cities, selected to be representative of the country's most populous and administratively significant areas and to encompass a wide range of climatic conditions. The latter, as well as hourly insolation throughout the year, results from ground measurements-based TMY (Typical Meteorological Year), used as an indicator of the most likely annual meteorological conditions. However, its accuracy in representing long-term climate characteristics depends also on the year-to-year consistency of climate parameters such as temperature and solar irradiation: the more stable these parameters remain from year to year, the more reliable the TMY is as a reference dataset. Any further in-depth analysis of the suitability of the TMY as a predictor for expected weather conditions should take into account not only the year-to-year variability from available datasets, but also the increasing frequency of extreme weather events and anomalous periods, which may challenge the validity of TMY-based analyses, especially in the context of climate change. The best tilt angle has been calculated by maximizing yearly insolation onto the tilted surface according to isotropic and anisotropic sky models, and by considering the results from selected online tools for comparison purposes (i.e. PVGIS and PVWatt). Although the best tilt is generally close to the local latitude angle, the study focused on the difference between these two angles (from here onward "latitude corrector"). The dependence of the latitude corrector on the climate conditions (i.e. seasonal and yearly clearness indexes) has been assessed, showing slight discrepancies between different sky diffuse models. Following the approach proposed in previous works, an analytical correlation has been proposed to calculate the latitude corrector as a function of selected independent variables: this relationship aimed to describe the optimum tilt angle for all examined areas while minimizing deviation from the "exact" value derived from the corresponding hourly TMY analysis. Results from Canadian cities have been compared to those from a similar analysis previously carried out by Memme and Fossa for France and Italy [51], thus highlighting the effect that peculiar climatic conditions at similar latitudes can have on solar energy harvesting. Finally, the analysis considered the effect of surface albedo on the yearly insolation: its value, often assumed equal to 0.2 for urban case studies, could be very different for cities for which a significant amount of snow is expected throughout the year. Considering an albedo equal to 0.8 when snow cover is reported by the TMY, as proposed in this analysis, can provide an estimation of how surrounding snow coverage modifies the optimum angles for PV installations and its overall effect on annual insolation.

2.1. Theoretical background

The optimum yearly tilt angle for fixed solar applications is defined as the angle that maximizes the annual global insolation on a tilted surface $H_{y,tot,T}$ (Eq. (1)). This insolation is considered a combination of beam ($H_{y,b,T}$), diffuse ($H_{y,diff,T}$) and reflected ($H_{y,ref,T}$) components [52].

$$H_{y,tot,T} = H_{y,b,T} + H_{y,diff,T} + H_{y,ref,T} \quad (1)$$

To maximize solar energy on a tilted surface, this study utilizes data for horizontal surfaces. Transposition models are employed to predict diffuse and reflected irradiance values. These models rely on a transposition factor, a non-dimensional ratio that depends on the solar position and system geometry, relating irradiance on the tilted surface to that on a horizontal one [3]. Diffuse insolation models are typically categorized as isotropic and anisotropic: isotropic models assume a uniform distribution of sky radiance, while anisotropic models account for variations in the diffuse fraction, including isotropic distribution, circumsolar radiation, and horizontal brightening. This study uses three models: the isotropic model by Liu and Jordan [53] and the two anisotropic models by Hay and Davies, both in their original form [54], and the improved HDKR (Hay, Davies, Klucher and Reindl) model [55]. These three approaches have been selected due to their ability to accurately represent the distribution of diffuse irradiance under various climatic conditions but also thanks to their relative simplicity and ease of integration with the available TMY data, which provides direct and diffuse irradiance values on horizontal surfaces.

A common feature of these models is the use of the beam insolation tilt factor, R_b, defined as the ratio of beam insolation on the tilted surface to that on a horizontal surface [56]. Various correlations exist in the literature to calculate the average value of this tilt factor over time intervals. In this research, the average tilt factor, $\overline{R}_b$, is expressed by Eq. (2) and depends solely on solar angles. The correlation is derived from the classic Duffie and Beckman reference [57], and uses two coefficients expressed in Eqs. (3) and (4). This correlation is valid when the hour angles at the initial (ω_1) and final (ω_2) time instants differ from the sunrise (ω_{sr}) and sunset (ω_{ss}) hour angles. It should be recalled that the hour angle ω represents the angular displacement of the sun relative to the local meridian, with 15° per hour (negative in the morning and positive in the afternoon). Other angles used as independent variables are:

- solar declination δ, assumed constant throughout single days;
- latitude φ;
- surface tilt angle β, as measured relative to the horizontal plane;
- surface azimuth angle γ, as measured from the north-south axis.

Some of these are schematically represented in Fig. 1, together with other solar angles of interest:

- the solar elevation angle α_s, measuring the angular position of the sun relative to the horizontal plane;
- its complement, the solar zenith angle θ_s, representing the angular position of the sun relative to the zenith direction;
- the solar azimuth angle γ_s, representing the horizontal angle of the sun's ground projection, measured from the south;
- the angle of incidence θ_w, Describes the angular position of the sun relative to the surface normal.

$$\overline{R}_b = \frac{a}{b} \quad (2)$$

$$\begin{aligned} a = {} & (\sin\delta \sin\varphi \cos\beta - \sin\delta \cos\varphi \sin\beta \cos\gamma) \cdot \frac{\pi}{180} \cdot (\omega_2 - \omega_1) \\ & + (\cos\delta \cos\varphi \cos\beta + \cos\delta \sin\varphi \sin\beta \cos\gamma) \cdot (\sin\omega_2 - \sin\omega_1) \\ & - (\cos\delta \sin\beta \sin\gamma) \cdot (\cos\omega_2 - \cos\omega_1) \end{aligned} \quad (3)$$

$$b = (\cos\varphi \cos\delta) \cdot (\sin\omega_2 - \sin\omega_1) + (\sin\varphi \sin\delta) \cdot \frac{\pi}{180} \cdot (\omega_2 - \omega_1) \quad (4)$$

According to the isotropic sky model proposed by Liu and Jordan (LJ), the global hourly insolation on a tilted surface is calculated according to Eq. (5), where ρ is the surface albedo.

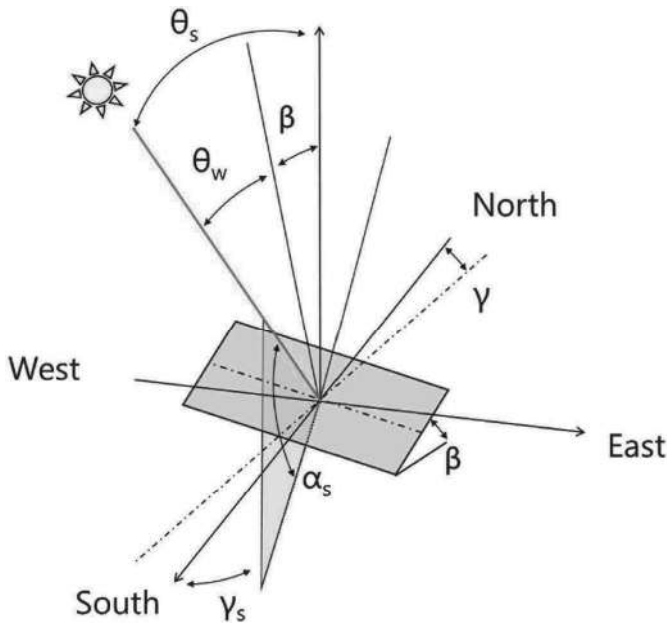

Fig. 1. Schematic representation of the main solar and surface angles.

$$H^{LJ}_{h,tot,T} = H_{h,b,H} \cdot R_b + H_{h,diff,H} \cdot \left[\frac{1+\cos(\beta)}{2}\right] \cdot + H_{h,tot,H} \cdot \rho \cdot \left[\frac{1-\cos(\beta)}{2}\right] \quad (5)$$

The Hay and Davies (HD) model is based on the assumption that the diffuse term can be represented by two factors, the isotropic and the circumsolar ones: this is specified by Eq. (6), where A_i is the anisotropy index, which determines the portion of the horizontal diffuse to be treated as forward scattered (Eq. (A3) in Appendix A).

$$\begin{aligned} H^{HD}_{h,tot,T} = {} & \left(H_{h,b,H} + H_{h,diff,H} \cdot A_i\right) \cdot R_b + H_{h,diff,H} \cdot (1 - A_i) \cdot \left[\frac{1+\cos(\beta)}{2}\right] \cdot \\ & + H_{h,tot,H} \cdot \rho \cdot \left[\frac{1-\cos(\beta)}{2}\right] \end{aligned} \quad (6)$$

Finally, according to the refined model known as HDKR (Eq. (7)), the horizon brightening factor is taken in consideration by means of the modulating factor *f* accounting for cloud cover (Eq. (A4) in Appendix A).

$$\begin{aligned} H^{HDKR}_{h,tot,T} = {} & \left(H_{h,b,H} + H_{h,diff,H} \cdot A_i\right) \cdot R_b + \\ & H_{h,diff,H} \cdot (1 - A_i) \cdot \left[\frac{1+\cos(\beta)}{2}\right] \cdot \left\{1 + f \cdot \left[\sin\left(\frac{\beta}{2}\right)\right]^3\right\} + H_{h,tot,H} \cdot \rho \cdot \left[\frac{1-\cos(\beta)}{2}\right] \end{aligned} \quad (7)$$

As mentioned in the Introduction section, the best tilt angle for PV surfaces is expected to show a dependence on average weather conditions. Consequently, in this paper, the clearness index K_t (Eq. (8)) is considered as an estimation of cloud cover, being calculated as the ratio of the average solar irradiance at ground level over a horizontal surface and the corresponding extra-terrestrial insolation $H_{h,tot,o}$ (Eq. (A2) in Appendix A).

$$K_t = \frac{H_{h,tot,H}}{H_{h,tot,o}} \quad (8)$$

A frequently used method for determining the optimum yearly tilt angle β at a specific city *i* is to express it as a linear function of the latitude, adjusted by a latitude corrector $\Delta\varphi$ (Eq. (9)). This angle can be either a constant or a variable dependent on specific relevant parameters usually derived from empirical data: typically, the smaller the geographical area of reference, the higher the accordance the optimum angle as calculated from analytical correlation (β*) and those estimated

from site-specific maximization of insolation on a tilted surface (β).

$$\beta^{*}_{opt,i} = \varphi_i - \Delta\varphi_i \tag{9}$$

2.2. Modelling

Starting from the TMY data, the hourly insolation on a south-facing inclined surface was calculated over an entire year: consequently, a set of three tilt angles was determined for each city, representing the angles that maximize the annual insolation according to the Liu & Jordan, Hay & Davies, and HDKR models, respectively. The calculation algorithm accounts for significant snow cover for extended periods in several cities. Specifically, the albedo was adjusted to alternate between two constant values based on the presence of snow, as indicated by the TMY data, following the approach adopted by Andrews et al. [58]. In this analysis, a standard albedo value of 0.2 is applied in the absence of snow, while snow cover results in an albedo of 0.8, in line with typical values reported in the literature [59]. However, it should be noted that snow albedo, which can exceed 0.8, may decrease due to factors such as melting, dust deposition, and reductions in snow depth. A comprehensive analysis of snow layer albedo is provided by Perovich [60].

Following the approach used by the authors for France and Italy [51], an analytical correlation was applied to calculate the optimum tilt angle based on monthly average insolation data. These data were derived from the TMY dataset as the daily average of hourly values, excluding records from intervals containing sunrise and sunset. It is important to note that calculating radiation on a tilted surface can be problematic near sunrise and sunset, as solar irradiance data may be recorded before sunrise or after sunset due to reflection from clouds or atmospheric refraction. To address this, the standard practice is to either discard these measurements or treat the radiation as entirely diffuse, as its impact on system performance is typically minimal: in this study, the criterion for selecting valid data was based on the hour angle ω. Only data corresponding to hour angles at least 15° greater than the sunrise hour angle (ω_{sr}) and at least 15° less than the sunset hour angle (ω_{ss}) were considered. This approach helps to avoid overestimations of the beam tilt factor R_b and eliminates potential negative values caused by approximations when converting local time to solar time and calculating the zenith angle during sunrise or sunset hours. Thus, Eq. (10) represents the daily average monthly value of total horizontal insolation, calculated using the complete TMY dataset. The same methodology was applied to both beam and diffuse components, where $H^{d}_{h,tot,H}$ represents the hourly total horizontal insolation during day *d*, and N^{month}_{day} denotes the total number of days in month *m*.

$$\overline{H}^{m}_{d,tot,H} = \frac{\sum_{d=1}^{d=N^{month}_{day}} \sum_{\omega=\omega_{d,sr}+15^{\circ}}^{\omega=\omega_{d,ss}-15^{\circ}} H^{d}_{h,tot,H}}{24 \cdot N^{month}_{day}} \tag{10}$$

In this research work, the optimum annual tilt angle was determined through a goal seek function: this has been performed for each city.

For the purposes of this analysis, an analytical correlation was used to express the latitude correction factor $\Delta\varphi$ as a function of latitude and clearness indices. For south-facing installations, two correlations demonstrated similar accuracy in predicting the optimum tilt angles, as shown in Eqs. (11) and (12). The first correlation involves only three numerical coefficients and yields an angular average standard deviation of 0.97 when compared to exact tilt values. The second correlation, which incorporates four numerical coefficients, provides slightly higher precision, with a standard deviation of 0.90. Based on results from similar studies, Eq. (12) is expected to perform better than Eq. (11) at different azimuth angles, so it will be used in the subsequent analyses.

$$w' = A'\left(1 - K_{t,w}/K_{t,s}\right) + B'\left(K_{t,y} - 1\right) + C'\varphi \tag{11}$$

$$w'' = A''\left(1 - K_{t,w}/K_{t,s}\right) + B''K_{t,y} + C''\varphi + D'' \tag{12}$$

2.3. Online tools

The PVWatts Calculator, developed by NREL, is an online tool used to estimate the energy production and cost savings of grid-connected PV systems. Widely used for initial assessments and feasibility studies for residential and commercial projects, PVWatts provides expected annual energy yields based on location, tilt angle, and azimuthal orientation of the PV system. The calculator uses weather data in the form of an hourly Typical Meteorological Year (TMY), sourced primarily from the NREL's National Solar Radiation Database (NSRDB) [61], and supplemented by other sources such as the Canadian Weather for Energy Calculations (CWEC). PVWatts calculates the beam, sky diffuse, and ground-reflected diffuse irradiance components on the PV module surface using the Perez 1990 algorithm [7]. Ground albedo values are taken from available weather files, or set to a default value of 0.2. The PVWatts Calculator was selected primarily due to its ability to estimate energy production and cost savings based on various locations and orientations, despite not directly providing the optimal tilt angle.

The Photovoltaic Geographical Information System (PVGIS), provided by the JRC (Joint Research Centre), is a web tool that offers solar irradiance data derived from satellite measurements. For North America, the PVGIS-NSRDB and PVGIS-ERA5 databases are used: the use of this database was motivated primarily by its high-resolution data for high-latitude cities, such as some of those in Canada. PVGIS-ERA5, a reanalysis product from the ECMWF (European Centre for Medium-Range Weather Forecasts), has a spatial resolution of 0.28° lat/lon and a temporal resolution of hourly data. The PVGIS tool allows for the estimation of yearly insolation on arbitrarily oriented surfaces and provides the best tilt angle for maximizing solar energy availability, which has been compared in this study to results from other methods.

3. The case study: reference cities and solar data sets

For the present analysis, solar radiation data derived from the Canadian Weather Year for Energy Calculation (CWEC) have been used [62]. This dataset has been recently updated to include a total number of 564 Canadian cities in the form of TMY files based on a database of up to 30 years of hourly values from the Canadian Weather Energy and Engineering Datasets (CWEEDS): solar data are from ground measurements or, if not available, from satellite-derived solar estimates. It should be stressed that the reliability of satellite data, such as those from PVGIS, to make energy production forecasts from PV plants has been widely assessed in the literature: an example is provided by the research done by González-Peña et al. [63], who compared results from a series of commercial and free software to real field data from three different PV plants For the aim of this study, TMY files for the most populous and capital cities have been selected for each province and territory, thus resulting in a total of 19 cities. Each file contains a series of hourly data, among which the following were considered for calculating the annual insolation and the best tilt angle for fixed PV applications: extraterrestrial irradiance $H_{h,tot,o}$ [kWh/m^2], global horizontal irradiance $H_{h,tot,H}$ [kWh/m^2], diffuse horizontal irradiance $H_{h,diff,H}$ [kWh/m^2] and snow cover, expressed as a dimensionless binary value. A short summary of the main geographical and weather values characterizing each city is provided in table form in Table 1.

As shown in Table 1, the complete set cities encompasses latitudes from 43.67° to 63.76°, ranging from yearly global insolation of 1345 kWh/m^2 to 913 kWh/m^2; comparing cities at the same latitude reveals how their climates exhibit site-specific peculiarities that are easily noticeable when considering the average clearness indexes, sunshine duration and the presence of snow. To mention a few examples, Quebec City stands out from other cities at similar latitudes due to a higher

Table 1
Summary of selected cities for PV best tilt analysis in Canada. Weather data from CWEC dataset [62].

City	Latitude [°]	Longitude [°]	$H_{y,tot,H}$ [kWh/m^2]	Kt_s	Kt_w	Kt_y	Sunshine duration [h]	Days with snow	Köppen climate classification
Toronto	43.67	−79.40	1345	0.54	0.41	0.48	3073	91	Dfb
Halifax	44.88	−63.51	1225	0.47	0.43	0.46	3075	90	Dfb
Ottawa	45.32	−75.67	1339	0.53	0.46	0.50	3102	110	Dfb
Montréal	45.47	−73.74	1340	0.53	0.46	0.50	3089	99	Dfb/Dfa
Fredericton	45.87	−66.54	1275	0.50	0.46	0.49	3067	105	Dfb
Moncton	46.11	−64.68	1232	0.48	0.45	0.47	3085	131	Dfb
Charlotteville	46.29	−63.12	1248	0.51	0.42	0.47	3032	117	Dfb
Québec City	46.80	−71.38	1297	0.52	0.45	0.49	3051	164	Dfb
St. John's	47.62	−52.75	1102	0.47	0.34	0.42	2825	129	Dfb
Victoria	48.65	−123.43	1237	0.54	0.36	0.46	2842	1	Csb/Dfb
Vancouver	49.19	−123.18	1244	0.57	0.35	0.46	2769	7	Cfb/Dfb
Winnipeg	49.91	−97.24	1274	0.53	0.48	0.51	3069	127	Dfb
Regina	50.43	−104.67	1322	0.56	0.51	0.54	3151	107	Dfb
Calgary	51.11	−114.02	1283	0.55	0.52	0.54	3115	96	Dfb/Dfc
Saskatoon	52.17	−106.70	1264	0.56	0.49	0.53	3032	123	Dfb
Edmonton	53.31	−113.58	1232	0.56	0.50	0.53	3021	136	Dfb
Whitehorse	60.71	−135.07	990	0.49	0.41	0.47	2711	191	Dfc
Yellowknife	62.46	−114.44	1029	0.54	0.40	0.48	2635	193	Dsb
Iqaluit	63.76	−68.56	913	0.48	0.41	0.46	2568	243	ET

occurrence of snowy days, while Victoria and Vancouver, with their more oceanic climate, experience lower snowfall. Regarding clear sky occurrences, Ottawa, Regina, and Calgary exhibit the highest levels of solar radiation and sunshine duration. In addition, seasonal climate trends can be investigated by comparing the clearness index *Kt* calculated as a 365-day average (Kt_y), the summer (Kt_s) and winter (Kt_w) indexes are calculated based on May to August and November to February values (Fig. 2).

Table 1 summarizes the climate of each city according to the widely recognized Köppen climate classification system [64]. This classification divides Earth's climates into five main groups, which are further subdivided based on patterns of seasonal precipitation and temperature. The majority of the cities fall under the humid continental category, with distinctions based on the presence of a dry season and the nature of the summer (Dfa, Dfb, Dsb). Additionally, there are occurrences of other climate types, including warm summer Mediterranean (Csb), regular subarctic (Dfc), oceanic (Cfb), and tundra (ET) climates.

4. Results and discussion

In this section, the results of the analysis are presented and discussed in detail. Section 4.1 focuses on the yearly insolation results derived from the three different sky models, with an emphasis on how the description of the diffuse component of solar radiation influences the outputs. Section 4.2 provides an analysis of the optimal tilt angles, comparing the latitude corrector obtained from the aforementioned sky models with the results from selected online tools. In Section 4.3, the accuracy of the proposed analytical correlation is evaluated by comparing the calculated results with those derived from tilt optimization. A discussion on the comparison between these results and similar analyses conducted for Italy and France is provided in Section 4.4, aimed at further assessing the general reliability of the model. Finally, Section 4.5 presents the findings from a variable albedo analysis, highlighting how snow cover may increase insolation on the tilted surface and modify the optimum tilt angle.

4.1. Yearly insolation from different diffuse sky models

This section presents the results of the analysis from the perspective of the annual insolation obtained using each of the three models for total insolation on an inclined surface, i.e. the isotropic Liu&Jordan model, the anisotropic model by Hay&Davies and its further improved version HDKR. Here the tilt angle has been optimized for each city to maximize the energy available by means of a GRG (Generalized Reduced Gradient) nonlinear optimization algorithm, available in spreadsheet tools for easy accessibility. The variation in insolation due to the type of model used is clearly greater for anisotropic models. Specifically, the Hay-Davies model results in values that are 2.7 %–5.6 % higher compared to the isotropic approach, while the more comprehensive HDKR model, which also considers the horizon brightening component, provides estimates that are 3.0 %–6.8 % higher. These discrepancies, when analyzed concerning the main variables introduced previously (i.e. latitude, seasonal and yearly clearness indexes), are strongly correlated with latitude, with correlation coefficients r of 0.88 and 0.89, respectively.

Based on these results, the annual average value of the *Rb* coefficient was considered to identify cities where the use of inclined surfaces has the greatest impact on total energy production. Referring to the HDKR model, it was found that the annual *Rb* is correlated with latitude with a correlation coefficient *r* of 0.71, ranging from a minimum value of 1.14 (St. John's) to a maximum of 1.37 (Yellowknife). The daily or monthly trends of these variables show higher values during the winter months, while horizontal surfaces would provide higher insolation during the

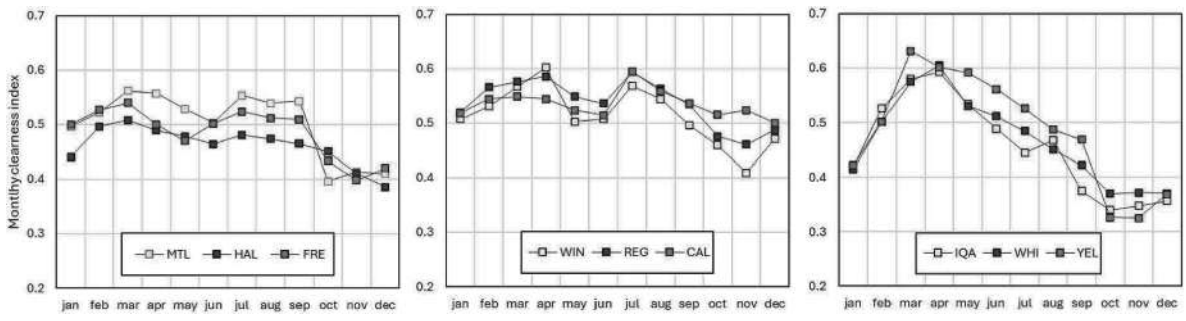

Fig. 2. Monthly average Kt index for a subset of cities in Canada as calculated from CWEC datasets [62].

summer months, characterized by clear skies and high solar elevation. In absolute terms, comparing the insolation on an inclined surface resulting from the HDKR model with that on a horizontal surface, as available from Table 1, annual increases range between 151 kWh/m^2 (St. John's) and 402 kWh/m^2 (Edmonton).

4.2. Latitude corrector $\Delta\varphi$: comparison between present model and online tools

In this section, the relationship between $\Delta\varphi$ and the variables of latitude, annual clearness index, and seasonal clearness indices – considered as the ratio between winter and summer values – was evaluated. Table 2 summarizes the r correlation coefficient values for each of the models considered, as well as the optimum angles obtained from the PVGIS and PVWatt portals. The last column represents the values from the previous analysis concerning France and Italy, involving the isotropic model [51].

The correlation analysis highlights that the key environmental factors influencing the optimum tilt angle have a significant variation across the selected calculation approaches. The most accurate sky model, i.e. the anisotropic HDKR, shows a prevailing correlation between the latitude corrector $\Delta\varphi$ and the ratio between winter and summer clearness indexes, as an indicator of seasonal climate variability (−0.83): in other words, the more the climate conditions vary significantly throughout the year (i.e. low values of the mentioned ratio), the more the best tilt differs from latitude. Similar considerations apply also to the correlation with yearly average clearness index, which should be considered as an indicator of to which extent climate conditions differs from clear sky, although the table highlights a less strong correlation. In general, latitude has a lower, positive, correlation with the latitude corrector $\Delta\varphi$ for the two anisotropic models, and this is even more evident with respect to the isotropic Liu and Jordan, as also confirmed by the corresponding results obtained in reference paper [51] for France and Italy. In high-latitude regions, especially during winter months, the sun position is described by lower altitude angles (α_s): this low solar angle leads to a specific distribution of sunlight across the sky that deviates from the uniform spread assumed in isotropic models like the Liu&Jordan one, that could potentially underestimate the tilt angle needed to best harvesting of solar energy in these conditions. Regarding the two selected web-app for best tilt calculation, while PVGIS shows similar correlations with the considered parameters, PVWatt results appear to be mainly based on latitude-dependent tilt corrections, less able to identify the variability in diffuse radiation's directional components due to yearly-average and seasonally-dependent clearness indexes.

Subsequently, the monthly average daily values for direct and diffuse insolation were calculated according to Eq. (10). Regarding the calculation of the best tilt angle, shown in Fig. 4, the two approaches, i.e. based on the maximization of hourly and daily average monthly sum respectively, yield essentially identical results for each diffuse radiation model, except for cities characterized by high latitudes. Indeed, for cities on the left-hand side of Fig. 3, the red results (HDKR) are quite comparable, and similarly for the blue (Hay and Davies) and yellow (Liu and Jordan) ones.

Comparing the results of this analysis with those obtained from the two online tools used as references, it is evident that PVWatt generally provides $\Delta\varphi$ values similar to those derived from the isotropic model, with notable deviations for latitudes above approximately 50°, the last three cities; in particular, for higher latitudes, $\Delta\varphi$ values can exceed 20°. Conversely, the output from PVGIS (in light grey) often overlaps with the results obtained from anisotropic models. Nevertheless, there are cases where the correction proposed by PVGIS is the lowest among those examined: these values never exceed 12°. However, it is important to note that the cities of Whitehorse and Yellowknife are outside the database used by the tool. Ultimately, the two online tools provide results that differ from each other by an average of 6°.

Regarding the analysis of the complete TMY, the isotropic approach, as expected, yields the highest correction values for $\Delta\varphi$. This is because a less refined analysis of the diffuse component tends to favor the direct component, and thus, insolation contributions associated to those sun positions characterized by higher solar elevation angles α_s. Consequently, a "summer" solution is more advantageous, with modules inclined at lower angles and positioned more horizontally. The anisotropic models, which consistently provide lower $\Delta\varphi$ values (with an average difference of 3.5°), offer a more accurate description of the diffuse component. The results from the Hay & Davies model show values ranging from 5.6° to 14.4°, while the HDKR model provides results for $\Delta\varphi$ between 3.7° and 13.2°, with optimum tilt angles being greater according to the HDKR model for all cities considered.

4.3. Analytical correlation for best tilt

This section presents the results derived from applying the previously introduced approximation correlation for latitude corrector $\Delta\varphi$ (Eq. (12)). The equation and the optimized set of coefficients were obtained for each of the diffuse insolation models by minimizing the difference between the annual insolation values from the monthly analysis and those obtained from the analytical calculation of the optimum tilt. Table 3 summarizes the values of the four coefficients associated with each transposition model: the complete sets of results used for this aim are provided in the Appendix in Tables B1, B2 and B3 (column β_{opt}, ρ = 0.2).

In Fig. 5, the results in terms of the best tilt obtained from the proposed correlation are graphically compared with the exact values calculated by maximizing insolation. In all three cases, the correlation coefficient r exceeds 0.98, effectively confirming the validity of the analytical formula regardless of the diffuse radiation model considered. To further assess the accuracy of the proposed correlation, the mean (μ) and standard deviation (σ) of the differences between the two sets of tilt angles (i.e. those obtained through the analytical correlation and those derived from the optimization process) are evaluated. To provide a comprehensive representation of variability, the confidence interval corresponding to $\mu \pm 2\sigma$ is reported, encompassing approximately 95 % of the observed differences. A summary of the results is presented in Table 4.

4.4. Comparison with European cities

The final part of this analysis includes a comparison between the results obtained for the European case study, which is based on numerous cities in France and Italy [51] and the current North American case study, which relies on a more limited database of cities in Canada. The objective of this comparison is to highlight how the optimum tilt angle must be determined by considering not only latitude but also

Table 2
Correlation coefficient r between latitude corrector Δφ, latitude and clearness indexes.

	Online tools		Isotropic model		Anisotropic models	
	PVGIS	PVWatt	Liu&Jordan	FRA + ITA	Hay&Davies	HDKR
$\Delta\varphi/\varphi$	0.57	0.88	0.34	0.39	0.57	0.59
$\Delta\varphi/Kt_y$	−0.38	−0.31	−0.73	−0.59	−0.65	−0.65
$\Delta\varphi/(Kt_w/Kt_s)$	−0.64	−0.45	−0.89	−0.82	−0.81	−0.83

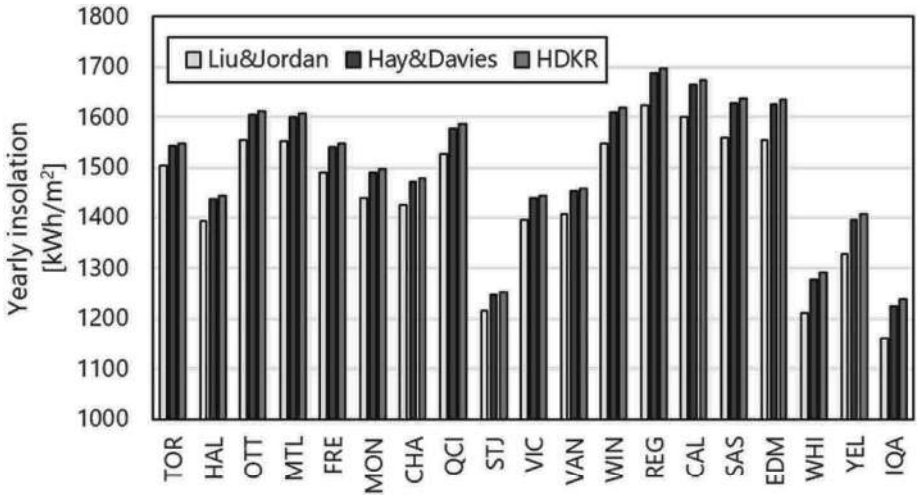

Fig. 3. Yearly insolation on best-tilted surfaces according to the three considered models. Cities are ordered according to their latitude.

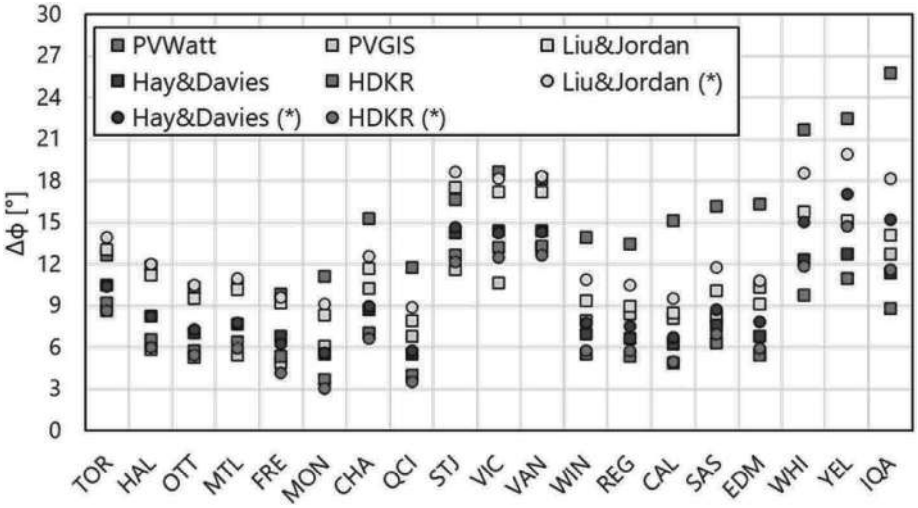

Fig. 4. Latitude corrector Δφ according to different approaches for best tilt calculation: (*) indicates results from daily average monthly values. Cities are ordered according to their latitude.

Table 3
Coefficients for best tilt calculation and correlation coefficients between tilts series calculated by solver and by the present formula.

Coefficient	Liu&Jordan	Hay&Davies	HDKR
A''	24.08	22.70	26.39
B''	39.96	32.68	18.49
C''	−0.34	−0.37	−0.32
D''	−11.89	−3.79	3.20

site-specific climatic conditions. This demonstrates that, even at the same latitude, different optimum angles can be obtained.

As shown in Fig. 6, the various data sets exhibit a strong underlying consistency, which can be attributed to the use of common assumptions and the same algorithm for calculating the optimum tilt angle. Here, the Liu Jordan (LJ) and Hay-Davies (HD) models are used for both European (triangular points) and Canadian (circular points) cities. Fig. 6 stresses quite obviously for the group of Canadian cities located at similar latitudes (nearly vertical alignments), that the use of accurate climatic data is crucial for properly setting up the optimization problem in analyses of this type. This is observed for nearly all latitudes between 45° and 65°.

4.5. Comparison with constant-albedo approach

One of the key findings of this analysis is the comparison of annual insolation, expressed in kWh/m^2/year, under two different methodologies: one assuming a fixed albedo value of 0.2 and the other incorporating a variable albedo based on snow presence. The latter consistently yields higher insolation due to the increased reflectance from snow-covered surfaces. The results highlight the potential errors in tilt calculations that may arise from inaccurately estimating the average ground albedo. Specifically, when optimum tilt is calculated using a constant albedo approach, neglecting the beneficial effects of snow coverage on winter irradiance, annual insolation outputs from the two methodologies may differ by up to 3.6 % in high-latitude cities. Even in lower-latitude areas, such as Quebec City, considering snow can result in a 1.8 % increase in insolation. It is important to note that this difference could be even greater if the insolation values were derived from distinct optimum tilt sets, i.e. specifically, those calculated using a constant albedo versus those obtained through variable albedo analysis. While this further difference generally ranges from 0.1 % to 0.2 %, it peaks at 0.3 % in Quebec City (overall 2.4 % increase) and 0.4 % in Iqaluit (where improved yearly tilt could yield up to 4.1 % more insolation than simple constant albedo optimum tilt (Fig. 7). This clearly addresses the need for

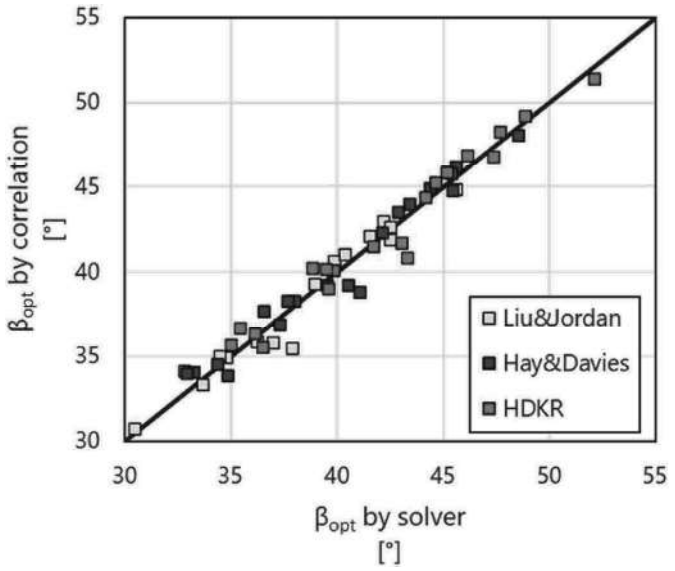

Fig. 5. Best tilt from insolation maximization ("by solver") and from present correlation.

Table 4
Mean (μ) and 95 % confidence interval (2σ) of the differences between tilt angles from the correlation and solver.

Statistical Metrics	Liu&Jordan	Hay&Davies	HDKR
μ [°]	0.47	0.56	0.58
2σ [°]	1.37	1.50	1.53

a refined tilt analysis that incorporates parameters related to average ground albedo. To direct the reader's attention to cities with the highest tilt variation, Fig. 8 illustrates the differences in the latitude corrector $\Delta\varphi$ based on the two approaches. It highlights areas where significant tilt adjustments are necessary, ranging from 0° (Victoria) to 7° (Iqaluit), with the variable albedo scenario obviously resulting in lower tilt angles. These results can also be compared to annual solar energy flux availability as calculated by the commonly used "latitude-based" approach, where tilt angles are set to match the latitude or adjusted by a fixed correction (e.g., 5°). The full set of results, detailed in Appendix B, demonstrates that an optimized tilt strategy can yield up to a 4 % increase in annual insolation, with respect to more traditional approaches, for medium-latitude cities. Additionally, these outputs help to identify cities and climate conditions where rule-of-thumb methods, such as simple latitude-based tilts, still provide a high degree of accuracy in determining the optimum fixed tilt angle. It should also be stressed that such a tilt optimization results in a reduction in the LCOE for the installation, provided that cost functions and conversion efficiencies are not dependent on the installation's tilt.

4.6. Discussion

The present analysis focuses on determining the optimal tilt angle to maximize front-side irradiance in monofacial PV systems. However, under specific conditions, this approach may not always lead to the most optimal solution: several factors can influence the actual best tilt angle, depending on the characteristics of the PV application, such as whether it is designed for utility-scale deployment or urban environments.

Some of the possible scenarios in which the best tilt angle might differ from the one proposed in this study include shading effects and environmental factors such as soiling and snow accumulation. Seasonal shading from surrounding buildings, mountains, or other obstacles may require site-specific optimization. A steeper tilt angle can mitigate shading from low obstacles (e.g., parapets or short barriers), while a shallower tilt may help reduce shading from taller structures. In urban environments, solar cadasters can be valuable for assessing partial shading and optimizing system design accordingly [65]. Furthermore, environmental factors such as soiling and snow accumulation should also be considered. In areas with high dust accumulation (e.g., deserts or urban settings), a steeper tilt angle can enhance self-cleaning effects, reducing energy losses due to soiling [66]. In regions with frequent snow accumulation, increasing the tilt angle can help minimize snow coverage and maintain energy yield [58]. It is also important to note that bifacial PV systems require a slightly different formulation of the optimization problem, as both front- and rear-side irradiance need to be considered: the optimal tilt or tracking strategy for bifacial systems depends not only on direct and diffuse radiation but also on ground albedo and the system's geometrical configuration [67].

Conclusions

This study provides a detailed analysis of optimum tilt angles for fixed PV installations across 19 Canadian cities, taking into account variations in sky radiation models and local climate conditions. Utilizing both isotropic and anisotropic models (Hay-Davies and HDKR), the results demonstrate that accurate modelling of diffuse radiation, especially in areas with seasonally variable weather, substantially affects both annual insolation and optimum tilt calculations. The first processing of data derived from CWEC portal reveals that the HDKR model, by considering horizon brightening, consistently yields annual insolation values 3.0 %–6.8 % higher than those predicted by isotropic models: these discrepancies show a strong correlation r with latitude, for both the HDKR (0.88) and Hay and Davies (0.89) models. One major methodological element in this work is the use of a variable albedo to account

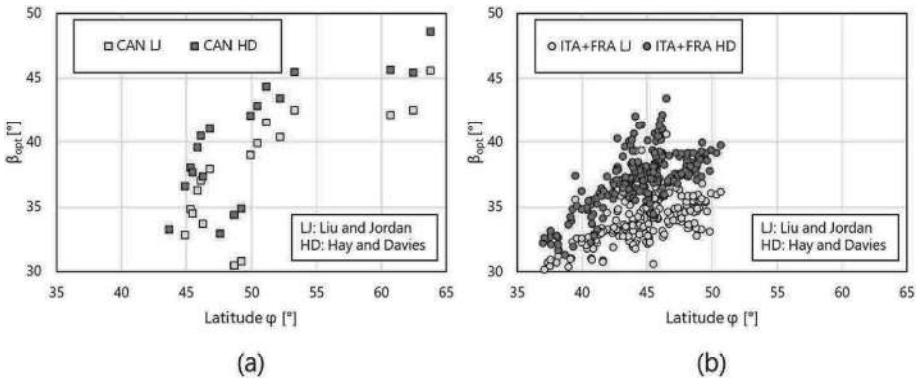

Fig. 6. Comparison between best tilts from the present Canadian case study (a) with those from selected cities in Italy and France (b) according to Liu-Jordan (LJ) and Hay-Davies (HD) models.

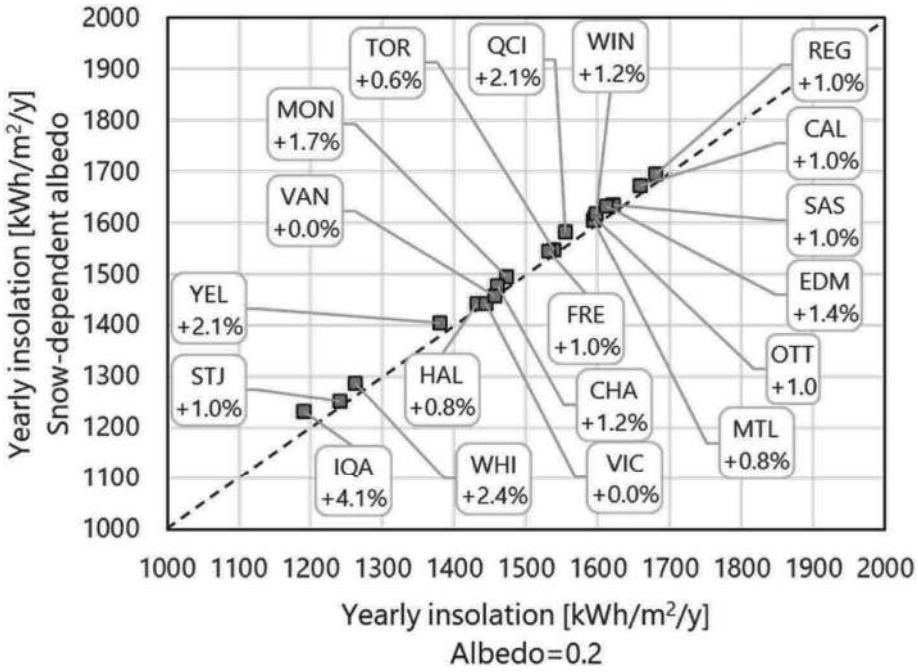

Fig. 7. Comparison between yearly insolation values: tilts are calculated according to the two presented approaches for albedo estimation; percentage differences indicate the increase in insolation when snow cover is accounted for.

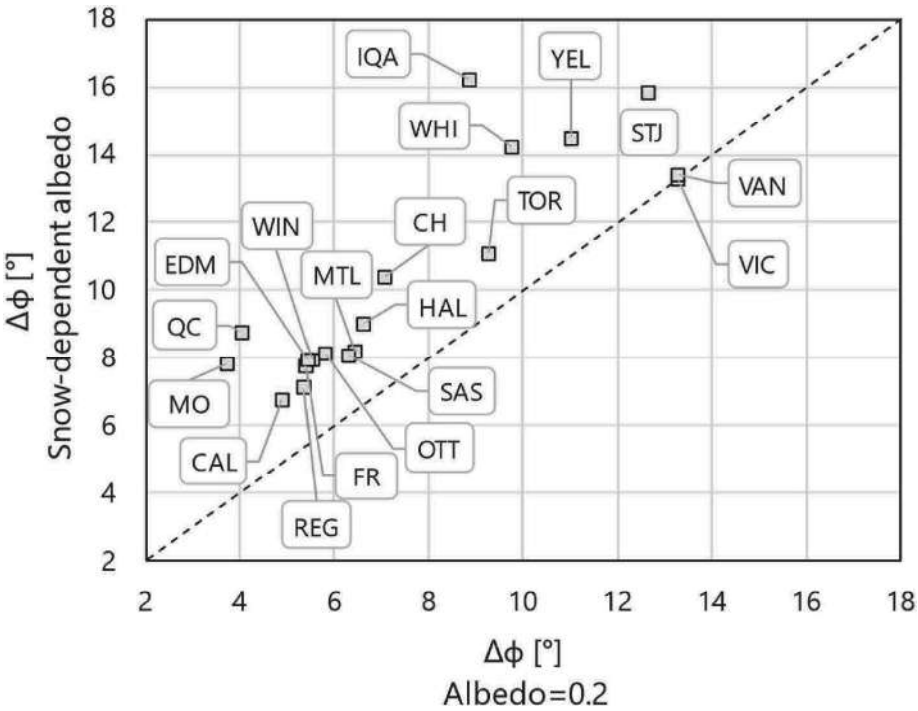

Fig. 8. Comparison between the two sets of latitude correctors Δφ optimized according to the two presented approaches for albedo estimation.

for snow cover. With albedo adjusted between 0.2 (no snow) and 0.8 (snow cover), the model reflects real-world conditions in snowy regions more accurately. This adjustment leads to annual insolation differences of up to 3.6 % between the variable and constant albedo approaches, with notable increases in insolation for cities such as Quebec City (+1.8 %) and Iqaluit (+4.1 %). The optimum tilt angles calculated with variable albedo generally trend lower than those with constant albedo, with differences reaching up to 5° in snow-prone regions. In terms of optimizing PV design, the introduction of a latitude corrector angle $\Delta\varphi$, correlated with both latitude and clearness indices, proved highly effective. This corrector angle, expressed by means of a properly defined analytical correlation, yielded a correlation coefficient above 0.98 compared to exact tilt values. The complete set of findings highlights that an optimized tilt strategy, following a variable albedo approach, can yield up to a 3.5 % gain in annual insolation relative to standard latitude-based installations, at latitudes lower than 60°. The expected gain is even greater for the more northern cities (up to 7.1 %), thus emphasizing the importance of incorporating local climate factors, such

as seasonal variability and snow cover, in PV system design.

CRediT authorship contribution statement

Samuele Memme: Writing – original draft, Visualization, Validation, Software, Investigation, Formal analysis, Data curation. **Marco Fossa:** Writing – review & editing, Supervision, Methodology, Investigation, Conceptualization. **Daniel Rousse:** Writing – review & editing, Supervision, Resources, Methodology, Conceptualization.

Declaration of generative AI and AI-assisted technologies in the writing process

During the preparation of this work the author(s) used ChatGPT in order to improve the English language and clarity of the manuscript. After using this tool/service, the author(s) reviewed and edited the content as needed and take(s) full responsibility for the content of the publication.

Declaration of competing interest

The authors declare that they have no known competing financial interests or personal relationships that could have appeared to influence the work reported in this paper.

Acknowledgements

The Authors acknowledge Professor Louis Lamarche, Director of the Département de génie mécanique, for invitation and support during S. Memme research period at the École de technologie supérieure, Montréal, Canada.

This work was partially carried out within the framework of the PNRR NEST Spoke 8 project (CUP D33C22001330002), which is gratefully acknowledged for its support.

The authors would also like to express their gratitude to Prof. Antonella Priarone for her valuable guidance and insightful discussions throughout the development of this work.

Appendix A

Equations for solar angles and insolation calculations, as derived from Ref. [57].

Declination angle:

$$\delta = 23.45^{\circ}\sin\left(360 \cdot \frac{284+n}{365}\right) \tag{A1}$$

Hourly extraterrestrial insolation on horizontal:

$$\overline{H}_{h,tot,o} = 1367 \cdot 3600 \cdot 24 \cdot \frac{1}{\pi}\left[1 + 0.033\cos\left(\frac{360n}{365}\right)\right]\left[\frac{\pi}{180}\omega_s \sin\varphi \sin\delta + \cos\varphi\cos\delta\sin\omega_s\right] \tag{A2}$$

Anisotropy index:

$$A_i = \frac{H_{h,b,H}}{H_{h,tot,o}} \tag{A3}$$

Cloud cover modulating factor:

$$f = \sqrt{\frac{H_{h,b,H}}{H_{h,tot,H}}} \tag{A4}$$

Appendix B

Numerical results of the analysis in terms of tilt angles and insolation values.

Table B1
Tilt angles and insolation values according to Liu and Jordan sky model

	β_{opt}, $\rho = 0.2$		β_{opt}, $\rho = 0.2/0.8$		$\beta = \varphi$, $\rho = 0.2$		$\beta = \varphi$-5°, $\rho = 0.2$	
	Tilt [°]	Insolation [kWh/m^2/y]	Tilt [°]	Insolation [kWh/m^2/y]	Tilt [°]	Insolation [kWh/m^2/y]	Tilt [°]	Insolation [kWh/m^2/y]
TOR	29	1495	31	1503	44	1461	39	1480
HAL	32	1385	34	1394	45	1360	40	1375
OTT	34	1542	36	1555	45	1518	40	1534
MTL	34	1541	35	1551	45	1517	40	1533
FRE	34	1478	37	1490	46	1457	41	1471
MON	34	1419	38	1439	46	1398	41	1412
CHA	32	1411	35	1425	46	1380	41	1398
QCI	34	1500	39	1527	47	1475	42	1491
STJ	27	1205	30	1215	48	1157	43	1178
VIC	31	1395	31	1396	49	1353	44	1374
VAN	32	1407	32	1408	49	1364	44	1385
WIN	38	1530	41	1546	50	1507	45	1522
REG	40	1609	41	1623	50	1587	45	1603
CAL	41	1586	43	1600	51	1567	46	1581
SAS	40	1546	42	1560	52	1521	47	1538
EDM	42	1536	44	1555	53	1512	48	1528
WHI	40	1189	45	1212	61	1140	56	1161

(*continued on next page*)

Table B1 (*continued*)

	β_{opt}, $\rho = 0.2$		β_{opt}, $\rho = 0.2/0.8$		$\beta = \varphi$, $\rho = 0.2$		$\beta = \varphi$-5°, $\rho = 0.2$	
	Tilt [°]	Insolation [kWh/m^2/y]	Tilt [°]	Insolation [kWh/m^2/y]	Tilt [°]	Insolation [kWh/m^2/y]	Tilt [°]	Insolation [kWh/m^2/y]
YEL	44	1305	47	1329	62	1255	57	1278
IQA	42	1121	50	1160	64	1067	59	1089

Table B2
Tilt angles and insolation values according to the Hay and Davies sky model

	β_{opt}, $\rho = 0.2$		β_{opt}, $\rho = 0.2/0.8$		$\beta = \varphi$, $\rho = 0.2$		$\beta = \varphi$-5°, $\rho = 0.2$	
	Tilt [°]	Insolation [kWh/m^2/y]	Tilt [°]	Insolation [kWh/m^2/y]	Tilt [°]	Insolation [kWh/m^2/y]	Tilt [°]	Insolation [kWh/m^2/y]
TOR	32	1534	33	1543	44	1509	39	1525
HAL	35	1427	37	1438	45	1411	40	1422
OTT	36	1590	38	1605	45	1574	40	1586
MTL	36	1588	38	1600	45	1572	40	1585
FRE	37	1525	39	1540	46	1512	41	1523
MON	37	1467	41	1489	46	1453	41	1464
CHA	35	1455	38	1472	46	1434	41	1448
QCI	37	1548	41	1578	47	1531	42	1544
STJ	31	1237	33	1249	48	1199	43	1218
VIC	34	1439	34	1439	49	1406	44	1425
VAN	35	1452	35	1453	49	1419	44	1438
WIN	41	1591	43	1609	50	1575	45	1587
REG	42	1673	44	1688	50	1658	45	1670
CAL	43	1650	45	1665	51	1637	46	1648
SAS	43	1613	45	1628	52	1596	47	1609
EDM	44	1604	46	1625	53	1588	48	1600
WHI	44	1250	48	1277	61	1213	56	1232
YEL	46	1370	50	1396	62	1329	57	1350
IQA	46	1181	52	1226	64	1137	59	1157

Table B3
Tilt angles and insolation values according to the HDKR sky model

	β_{opt}, $\rho = 0.2$		β_{opt}, $\rho = 0.2/0.8$		$\beta = \varphi$, $\rho = 0.2$		$\beta = \varphi$-5°, $\rho = 0.2$	
	Tilt [°]	Insolation [kWh/m^2/y]	Tilt [°]	Insolation [kWh/m^2/y]	Tilt [°]	Insolation [kWh/m^2/y]	Tilt [°]	Insolation [kWh/m^2/y]
TOR	33	1538	34	1548	44	1519	39	1532
HAL	36	1432	38	1444	45	1420	40	1430
OTT	37	1595	40	1611	45	1583	40	1593
MTL	37	1594	39	1606	45	1582	40	1592
FRE	38	1531	40	1547	46	1521	41	1530
MON	38	1473	42	1498	46	1464	41	1472
CHA	36	1460	39	1478	46	1444	41	1456
QCI	38	1554	43	1586	47	1541	42	1552
STJ	32	1241	35	1253	48	1210	43	1226
VIC	35	1443	35	1444	49	1417	44	1433
VAN	36	1457	36	1457	49	1430	44	1446
WIN	42	1598	44	1618	50	1587	45	1597
REG	43	1681	45	1697	50	1671	45	1680
CAL	44	1658	46	1674	51	1649	46	1657
SAS	44	1621	46	1636	52	1608	47	1619
EDM	45	1612	48	1635	53	1601	48	1611
WHI	46	1261	51	1291	61	1234	56	1250
YEL	48	1379	51	1408	62	1347	57	1365
IQA	48	1191	55	1240	64	1158	59	1175

References

[1] G. Masson, M. de L'Epine, I. Kaizuka, PVPS trends in photovoltaic applications. www.iea-pvps.org, 2023.

[2] IRENA, Renewable capacity statistics 2022, Abu Dhabi (2022). https://www.irena.org/publications/2022/Apr/Renewable-Capacity-Statistics-2022. (Accessed 22 May 2023).

[3] D. Yang, Solar radiation on inclined surfaces: corrections and benchmarks, Sol. Energy 136 (2016) 288–302, https://doi.org/10.1016/j.solener.2016.06.062.

[4] A.K. Yadav, S.S. Chandel, Tilt angle optimization to maximize incident solar radiation: a review, Renew. Sustain. Energy Rev. 23 (2013) 503–513, https://doi.org/10.1016/J.RSER.2013.02.027.

[5] B.Y.H. Liu, R.C. Jordan, The interrelationship and characteristic distribution of direct, diffuse and total solar radiation, Sol. Energy 4 (1960) 1–19, https://doi.org/10.1016/0038-092X(60)90062-1.

[6] N. Bailek, K. Bouchouicha, N. Aoun, M. El-Shimy, B. Jamil, A. Mostafaeipour, Optimized fixed tilt for incident solar energy maximization on flat surfaces located in the Algerian big south, Sustain. Energy Technol. Assessments 28 (2018) 96–102, https://doi.org/10.1016/J.SETA.2018.06.002.

[7] R. Perez, P. Ineichen, R. Seals, J. Michalsky, R. Stewart, Modeling daylight availability and irradiance components from direct and global irradiance, Sol. Energy 44 (1990) 271–289, https://doi.org/10.1016/0038-092X(90)90055-H.

[8] K.N. Shukla, S. Rangnekar, K. Sudhakar, Comparative study of isotropic and anisotropic sky models to estimate solar radiation incident on tilted surface: a case study for Bhopal, India, Energy Rep. 1 (2015) 96–103, https://doi.org/10.1016/J.EGYR.2015.03.003.

[9] E. Calabrò, The disagreement between anisotropic-isotropic diffuse solar radiation models as a function of solar declination: computing the optimum tilt angle of solar panels in the area of Southern-Italy, Smart Grid and Renew. Energy 03 (2012) 253–259, https://doi.org/10.4236/sgre.2012.34035.

[10] A. Padovan, D. Del Col, Measurement and modeling of solar irradiance components on horizontal and tilted planes, Sol. Energy 84 (2010) 2068–2084, https://doi.org/10.1016/j.solener.2010.09.009.

[11] R. Posadillo, R. López Luque, Evaluation of the performance of three diffuse hourly irradiation models on tilted surfaces according to the utilizability concept, Energy Convers. Manag. 50 (2009) 2324–2330, https://doi.org/10.1016/j.enconman.2009.05.014.

[12] P.I. Raptis, S. Kazadzis, B. Psiloglou, N. Kouremeti, P. Kosmopoulos, A. Kazantzidis, Measurements and model simulations of solar radiation at tilted planes, towards the maximization of energy capture, Energy (Calg.) 130 (2017) 570–580, https://doi.org/10.1016/j.energy.2017.04.122.

[13] E. González-González, J. Martín-Jiménez, M. Sánchez-Aparicio, S. del Pozo, S. Lagüela, Evaluating the standards for solar PV installations in the Iberian Peninsula: analysis of tilt angles and determination of solar climate zones, Sustain. Energy Technol. Assessments 49 (2022) 101684, https://doi.org/10.1016/J.SETA.2021.101684.

[14] A. Barbón, C. Bayón-Cueli, L. Bayón, C. Rodríguez-Suanzes, Analysis of the tilt and azimuth angles of photovoltaic systems in non-ideal positions for urban applications, Appl. Energy 305 (2022) 117802, https://doi.org/10.1016/J.APENERGY.2021.117802.

[15] S. Yadav, C. Hachem-Vermette, S.K. Panda, G.N. Tiwari, S.S. Mohapatra, Determination of optimum tilt and azimuth angle of BiSPVT system along with its performance due to shadow of adjacent buildings, Sol. Energy 215 (2021) 206–219, https://doi.org/10.1016/J.SOLENER.2020.12.033.

[16] W.S. Ebhota, P.Y. Tabakov, Impact of photovoltaic panel orientation and elevation operating temperature on solar photovoltaic system performance, Int. J. Renew. Energy Dev. 11 (2022) 591–599, https://doi.org/10.14710/ijred.2022.43676.

[17] H. Moghadam, F.F. Tabrizi, A.Z. Sharak, Optimization of solar flat collector inclination, Desalination 265 (2011) 107–111, https://doi.org/10.1016/J.DESAL.2010.07.039.

[18] T.P. Chang, The Sun's apparent position and the optimal tilt angle of a solar collector in the northern hemisphere, Sol. Energy 83 (2009) 1274–1284, https://doi.org/10.1016/j.solener.2009.02.009.

[19] A. Luque, S. Hegedus, Optimal inclination angle versus latitude, in: Wiley (Ed.), Handbook of Photovoltaic Science and Engineering, Second Edi, 2011, pp. 1012–1020, https://doi.org/10.1002/9780470974704.

[20] A. Khosravi, O. Ricardo Sandoval Rodriguez, B. Talebjedi, T. Laukkanen, J. Jose Garcia Pabon, M. El Haj Assad, New correlations for determination of optimum slope angle of solar collectors, Energy Eng. J. Assoc. Energy Eng. 117 (2020) 249–265, https://doi.org/10.32604/EE.2020.011024.

[21] P. Talebizadeh, M.A. Mehrabian, M. Abdolzadeh, Determination of optimum slope angles of solar collectors based on new correlations, Energy Sources, Part A Recovery, Util. Environ. Eff. 33 (2011) 1567–1580, https://doi.org/10.1080/15567036.2010.551253.

[22] N. Nijegorodov, K.R.S. Devan, P.K. Jain, S. Carlsson, Atmospheric transmittance models and an of analytical model to predict the optimum slope of an absorber plate, variously oriented at any latitude, Renew. Energy 4 (1994) 529–543.

[23] H. Darhmaoui, D. Lahjouji, Latitude based model for tilt angle optimization for solar collectors in the mediterranean region, Energy Proc. 42 (2013) 426–435, https://doi.org/10.1016/J.EGYPRO.2013.11.043.

[24] D. Santos-Martin, S. Lemon, SoL – a PV generation model for grid integration analysis in distribution networks, Sol. Energy 120 (2015) 549–564, https://doi.org/10.1016/J.SOLENER.2015.07.052.

[25] M. Chinchilla, D. Santos-Martín, M. Carpintero-Rentería, S. Lemon, Worldwide annual optimum tilt angle model for solar collectors and photovoltaic systems in the absence of site meteorological data, Appl. Energy 281 (2021) 116056, https://doi.org/10.1016/J.APENERGY.2020.116056.

[26] M.Z. Jacobson, V. Jadhav, World estimates of PV optimal tilt angles and ratios of sunlight incident upon tilted and tracked PV panels relative to horizontal panels, Sol. Energy 169 (2018) 55–66, https://doi.org/10.1016/j.solener.2018.04.030.

[27] R. Abdallah, A. Juaidi, S. Abdel-Fattah, F. Manzano-Agugliaro, Estimating the optimum tilt angles for south-facing surfaces in Palestine, Energies 13 (2020) 623, https://doi.org/10.3390/en13030623.

[28] K. Skeiker, Optimum tilt angle and orientation for solar collectors in Syria, Energy Convers. Manag. 50 (2009) 2439–2448, https://doi.org/10.1016/j.enconman.2009.05.031.

[29] M. Benghanem, Optimization of tilt angle for solar panel: case study for Madinah, Saudi Arabia, Appl. Energy 88 (2011) 1427–1433, https://doi.org/10.1016/j.apenergy.2010.10.001.

[30] M. Abdolzadeh, M.A. Mehrabian, The optimal slope angle for solar collectors in hot and dry parts of Iran, Energy Sources, Part A Recovery, Util. Environ. Eff. 34 (2012) 519–530, https://doi.org/10.1080/15567036.2011.576413.

[31] R. Sadeghi, M. Parenti, S. Memme, M. Fossa, S. Morchio, A review and comparative analysis of solar tracking systems, Energies 18 (2025) 2553, https://doi.org/10.3390/en18102553.

[32] K. Bakirci, General models for optimum tilt angles of solar panels: turkey case study, Renew. Sustain. Energy Rev. 16 (2012) 6149–6159, https://doi.org/10.1016/J.RSER.2012.07.009.

[33] M. Tiris, C. Tiris, Optimum collector slope and model evaluation: case study for Gebze, Turkey, Energy Convers. Manag. 39 (1998) 167–172, https://doi.org/10.1016/S0196-8904(96)00229-4.

[34] M.A. Kallioğlu, A. Durmuş, H. Karakaya, A. Yılmaz, Empirical calculation of the optimal tilt angle for solar collectors in northern hemisphere, energy sources, part A: recovery, Utilization Environ. Effects 42 (2020) 1335–1358, https://doi.org/10.1080/15567036.2019.1663315.

[35] H.Z. Al Garni, A. Awasthi, D. Wright, Optimal orientation angles for maximizing energy yield for solar PV in Saudi Arabia, Renew. Energy 133 (2019) 538–550, https://doi.org/10.1016/j.renene.2018.10.048.

[36] A. Sharma, M.A. Kallioğlu, A. Awasthi, R. Chauhan, G. Fekete, T. Singh, Correlation formulation for optimum tilt angle for maximizing the solar radiation on solar collector in the Western Himalayan region, Case Stud. Therm. Eng. 26 (2021) 101185, https://doi.org/10.1016/J.CSITE.2021.101185.

[37] Q. Hassan, M.K. Abbas, A.M. Abdulateef, J. Abulateef, A. Mohamad, Assessment the potential solar energy with the models for optimum tilt angles of maximum solar irradiance for Iraq, Case Stud. Chem. Environ. Eng. 4 (2021) 100140, https://doi.org/10.1016/J.CSCEE.2021.100140.

[38] C. Stanciu, D. Stanciu, Optimum tilt angle for flat plate collectors all over the world – a declination dependence formula and comparisons of three solar radiation models, Energy Convers. Manag. 81 (2014) 133–143, https://doi.org/10.1016/J.ENCONMAN.2014.02.016.

[39] S. Soulayman, M. Hammoud, Optimum tilt angle of solar collectors for building applications in mid-latitude zone, Energy Convers. Manag. 124 (2016) 20–28, https://doi.org/10.1016/J.ENCONMAN.2016.06.066.

[40] H. Yang, L. Lu, The optimum tilt angles and orientations of PV claddings for building-integrated photovoltaic (BIPV) applications, J. Solar Energy Eng. Transact. ASME 129 (2007) 253–255, https://doi.org/10.1115/1.2212439.

[41] Y. Liu, L. Yao, H. Jiang, N. Lu, J. Qin, T. Liu, C. Zhou, Spatial estimation of the optimum PV tilt angles in China by incorporating ground with satellite data, Renew. Energy 189 (2022) 1249–1258, https://doi.org/10.1016/J.RENENE.2022.03.072.

[42] M.M. Elsayed, Optimum orientation of absorber plates, Sol. Energy 42 (1989) 89–102, https://doi.org/10.1016/0038-092X(89)90136-9.

[43] F. Jafarkazemi, S. Ali Saadabadi, H. Pasdarshahri, The optimum tilt angle for flat-plate solar collectors in Iran, J. Renew. Sustain. Energy 4 (2012), https://doi.org/10.1063/1.3688024.

[44] S. Soulayman, W. Sabbagh, Optimum tilt angle at tropical region, Int. J. Renew. Energy Dev. 4 (2015) 48–54, https://doi.org/10.14710/ijred.4.1.48-54.

[45] M.A.A. Mamun, R. Md Sarkar, M. Parvez, J. Nahar, M. Sohel Rana, Determining the optimum tilt angle and orientation for photovoltaic (PV) systems in Bangladesh. 2nd International Conference on Electrical and Electronic Engineering, ICEEE 2017, 2018, pp. 1–4, https://doi.org/10.1109/CEEE.2017.8412910.

[46] A.K. Yadav, S.S. Chandel, Formulation of new correlations in terms of extraterrestrial radiation by optimization of tilt angle for installation of solar photovoltaic systems for maximum power generation: case study of 26 cities in India, Sadhana - Acad. Proc. Eng. Sci. 43 (2018) 1–15, https://doi.org/10.1007/s12046-018-0858-2.

[47] L. Wenxian, Optimum inclinations for the entire year of south-facing solar collectors in China, Energy (Calg.) 14 (1989) 863–866, https://doi.org/10.1016/0360-5442(89)90040-6.

[48] C.B. Christensen, G.M. Barker, Effects of tilt and azimuth on annual incident solar radiation for United States locations, Int. Solar Energy Conf. (2001) 225–232, https://doi.org/10.1115/sed2001-128.

[49] A. Barbón, P.F. Ayuso, L. Bayón, C.A. Silva, A comparative study between racking systems for photovoltaic power systems, Renew. Energy 180 (2021) 424–437, https://doi.org/10.1016/j.renene.2021.08.065.

[50] A. Ferry, M. Parenti, M. Thebault, C. Ménézo, M. Fossa, Optimal tilt angles for bifacial photovoltaic plants across Europe based on cumulative sky and typical meteorological year data, Sol. Energy 293 (2025) 113475, https://doi.org/10.1016/j.solener.2025.113475.

[51] S. Memme, M. Fossa, Maximum energy yield of PV surfaces in France and Italy from climate based equations for optimum tilt at different azimuth angles, Renew. Energy 200 (2022) 845–866, https://doi.org/10.1016/j.renene.2022.10.019.

[52] J.A. Duffie, W.A. Beckman, Solar engineering of thermal processes. https://doi.org/10.1016/0142-694x(82)90016-3, 1982.

[53] B. Liu, R. Jordan, Daily insolation on surfaces tilted towards equator, ASHRAE 10 (1961) 53–59.

[54] J.E. Hay, J.A. Davies, Calculation of the solar radiation incident on an inclined surface, in: First Canadian Solar Radiation Data Workshop, Canadian Atmospheric Environment Service, 1980, pp. 59–72. Toronto.

[55] D.T. Reindl, W.A. Beckman, J.A. Duffie, Evaluation of hourly tilted surface radiation models, Sol. Energy 45 (1990) 9–17, https://doi.org/10.1016/0038-092X(90)90061-G.

[56] M.M. Rahman, S. Shareef, R. Rahman, M.G.M. Choudhury, Computation of solar radiation tilt factor and optimum tilt angle for Bangladesh, Indian J. Radio Space Phys. 29 (2000) 37–40.

[57] J.A. Duffie, W.A. Beckman, Solar Engineering of Thermal Processes, John Wiley & Sons, Inc., Hoboken, NJ, USA, 2013, https://doi.org/10.1002/9781118671603.

[58] R.W. Andrews, A. Pollard, J.M. Pearce, The effects of snowfall on solar photovoltaic performance, Sol. Energy 92 (2013) 84–97, https://doi.org/10.1016/j.solener.2013.02.014.

[59] E. Andenæs, B.P. Jelle, K. Ramlo, T. Kolås, J. Selj, S.E. Foss, The influence of snow and ice coverage on the energy generation from photovoltaic solar cells, Sol. Energy 159 (2018) 318–328, https://doi.org/10.1016/j.solener.2017.10.078.
[60] D.K. Perovich, Light reflection and transmission by a temperate snow cover, J. Glaciol. 53 (2007) 201–210, https://doi.org/10.3189/172756507782202919.
[61] M. Sengupta, Y. Xie, A. Lopez, A. Habte, G. Maclaurin, J. Shelby, The National Solar Radiation Data Base (NSRDB), Renew. Sustain. Energy Rev. 89 (2018) 51–60, https://doi.org/10.1016/j.rser.2018.03.003.
[62] Government of Canada, Canadian weather year for energy calculation (CWEC), natural resources Canada. https://open.canada.ca/data/en/dataset/55438acb-aa67-407a-9fdb-1cb21eb24e28, 2022. (Accessed 31 October 2024).
[63] D. González-Peña, I. García-Ruiz, M. Díez-Mediavilla, M.I. Dieste-Velasco, C. Alonso-Tristán, Photovoltaic prediction software: evaluation with real data from northern Spain, Appl. Sci. (Switzerland) 11 (2021), https://doi.org/10.3390/app11115025.
[64] H.E. Beck, N.E. Zimmermann, T.R. McVicar, N. Vergopolan, A. Berg, E.F. Wood, Present and future Köppen-Geiger climate classification maps at 1-km resolution, Sci. Data 5 (2018) 180214, https://doi.org/10.1038/sdata.2018.214.
[65] S. Memme, D. Lepore, A. Priarone, M. Fossa, Estimating the solar potential of the rooftops of the city of Genova through the 3D modelling of the built environment and anisotropic tiled sky analysis, J. Phys. Conf. Ser. 2893 (2024) 012121, https://doi.org/10.1088/1742-6596/2893/1/012121.
[66] T. Alkharusi, G. Huang, C.N. Markides, Characterisation of soiling on glass surfaces and their impact on optical and solar photovoltaic performance, Renew. Energy 220 (2024) 119422, https://doi.org/10.1016/j.renene.2023.119422.
[67] M. Parenti, S. Memme, M. Fossa, Sky radiance distribution based model for rear and front insolation estimation on PV bifacial modules, Sol. Energy Mater. Sol. Cell. 289 (2025) 113677, https://doi.org/10.1016/j.solmat.2025.113677.